applied sciences

MDPI

Article

Cytological Applications of the Vacuolization Phenomenon as a Means of Determining Saline Cytotoxicity

Onisan Emilian, Sarac Ioan *, Petrescu Irina *, Pascalau Raul, Ciulca Adriana, Camen Dorin and Stroia Ciprian

Genetic Department, University of Life Sciences "King Mihai I", 119 Calea Aradului Street, 300645 Timisoara, Romania; emilianonisan.sunflower@gmail.com (O.E.); raul.pascalau@usvt.ro (P.R.); adrianaciulca@usvt.ro (C.A.); dorincamen@usvt.ro (C.D.); ciprian.stroia@usvt.ro (S.C.)

* Correspondence: ioansarac@usvt.ro (S.I.); irinapetrescu@usvt.ro (P.I.)

Abstract: Salt stress induces cytotoxicity at the cellular level, influencing the vacuolization process, disrupting mitotic division, and thus inhibiting plant growth. The results for a range of species used in agriculture have shown that high soil salt levels affect germination, chlorophyl content and yield. In this study, an experiment was carried out in the laboratory using NaCl concentration treatments of 0, 100, 125 and 150 mM on sunflower seeds of the inbred line HA-89 obtained from the USDA gene bank. For the experiment, the seeds were germinated in a salt solution and analyzed cytologically by calculating the mitotic index, chromosomal aberration index, provacuolar index and vacuolization index. Following our cytological studies, we observed that the vacuolization phenomenon was caused by salt stress and progressively accentuated by the salt concentration levels and exposure times. The formation of vacuolized cells is due to the fusion of provacuoles, which contributes to a uniform or non-uniform distribution of genetic material around them. According to our results, the vacuolization index showed high values depending on the NaCl concentration and stress exposure time. Similarly, high salt concentrations significantly decreased the mitotic index and increased the chromosomal aberration index. The effect of salt stress causes cell vacuolization, a decrease in the mitotic index and an increase in the number of chromosomal aberrations in meristematic tissues, inhibiting growth and development and consequently leading to a reduction in productivity per unit area.

Keywords: salt stress; vacuole; cytotoxicity; vacuolization; mitotic index; chromosomal aberrations

Citation: Emilian, O.; Ioan, S.; Irina, P.; Raul, P.; Adriana, C.; Dorin, C.; Ciprian, S. Cytological Applications of the Vacuolization Phenomenon as a Means of Determining Saline Cytotoxicity. *Appl. Sci.* **2023**, *13*, 8461. https://doi.org/10.3390/app13148461

Academic Editor: Marco G. Alves

Received: 6 June 2023
Revised: 8 July 2023
Accepted: 18 July 2023
Published: 21 July 2023

1. Introduction

Salt concentration in saline soils has a negative effect on the biochemistry, anatomy and productivity of plants [1–5]. The increasing concentration of salt in soils is causing a considerable loss of agricultural potential worldwide, covering around 15% of the total agricultural area due to its increasing extent [6]. Salt and drought stress influence the accumulation of osmolytes and antioxidant compounds, such as flavonoids, at the cellular level. The stress effect of different concentrations of NaCl reduces the amount of chlorophyll, unlike drought stress [7]. Researchers have shown that high concentrations of NaCl decrease the mitotic index and increase the number of chromosomal aberrations [8,9]. In addition, the effect of different amounts of NaCl leads to altered metabolic functions in plant tissues and a reduction in flavonoids [10]. Some studies have shown that foliar application of KNO_3 fertilizer has positive effects in combating salt stress [11]. These positive effects on NaCl stress have also been demonstrated using agmatine treatments [12]. Phytohormones also play an important role in abiotic stress tolerance, including salt tolerance. Previous studies have shown that the application of salicylic acid improved the growth of maize plants under salt stress [13,14].

Several studies indicate that the effect of salt stress plays a role in the accumulation of reactive oxygen species (ROS), which leads to abnormalities in cellular cycles and influences plant growth [15–17].

Current research indicates a correlation between the increased accumulation of ROS and programmed cell death (PCD) in response to the effect caused by saline solutions [18,19]. A cytological phenomenon correlated with abiotic or biotic stress in plant cells has been observed in the form of irreversible vacuolization of the cells. The initial physiological signal of vacuolization is determined by the presence of a greater number of provacuoles in plant cells when osmotic processes malfunction [20,21].

Salt stress influences the vacuole formation process in plants cells [22]. However, vacuolization also occurs in animal cells in response to stress caused by various chemicals or by viral or bacterial infections [23]. Concerning studies showing that vacuolization is a characteristic phenomenon in the identification of cellular stress, including salt stress, numerous authors have described vacuolization in response to various stress factors in rice [24], wheat [25], vegetables [26], cotton [27], rapeseed [28], soybean [29] and maize [30]. Researchers have also observed that diets containing oil from the world's three main oil crops—rapeseed [31], soybean [32] and sunflower [33]—induced hepatocyte vacuolization.

The sunflower (*Helianthus annuus* L.) belongs to the *Asteraceae* family, and it is known for its quality and ease of oil extraction compared to other oilseed species [34]. The sunflower crop is used not only for oil extraction but also for seed production in human food [35–37] and as an ornamental plant [38]. All these reasons have led to the very large-scale cultivation of this species. Current sunflower breeding programs focus on the development of new genotypes, using in vitro biotechnology to develop genotypes tolerant to salt stress [39].

The aim of this research was to elucidate cellular physiological activities that can be used as starting points for identifying sunflower genotypes tolerant to different stresses, especially NaCl, in sunflower breeding programs. Cytological examinations of sunflowers and the use of biotechnological methods in sunflower breeding programs enable rapid cytological diagnosis and the selection of genotypes tolerant to salt stress. Vacuolization has not been used at all as a breeding method, nor has it been established whether it occurs under salt stress in the sunflower. In addition, this research will open new horizons of research in the future to determine the correlation between other stress factors and seed oil content in the vacuolization phenomenon.

2. Materials and Methods

2.1. Plant Germplasm

For this experiment, we selected the inbred line HA-89 of *Helianthus annuus* L. Seeds were obtained from USDA germplasm stocks. The sunflower line HA-89 is an inbred line developed in 1975 in Texas and maintained at North Central Regional under the code Pl 599773. The weight of 1000 seeds (MMB) was 60.2 g, with an oil content of 41%, of which 57% was linoleic acid, 37% was oleic acid and the remaining 10% was other unsaturated oils.

2.2. Sterilization and Germination Conditions

Seeds were sterilized by immersing them for 15 m in a 0.1% mercury chloride solution ($HgCI_2$). To drain the $HgCl_2$ sterilization solution, sunflower seeds were washed in five baths of distilled water for 3 min each. Sterilized sunflower seeds were germinated in distilled water and various saline solutions on filter paper in 12 cm Petri dishes at 25 °C ± 5 under a photoperiod of 16 h day plus 8 h night.

2.3. Experimental Design

The experiment was carried out by treating 25 sunflower seeds of each experimental variant. The study was repeated three times to observe the cytological phenomena. Sunflower seeds were germinated at concentrations of 0 nM (control V1), 100 mM (V2), 125 mM (V3) and 150 mM (V4) NaCl. The experiment lasted 13 days, including the 3–5-day germination period, during which secondary root formation was induced on day 10 by removing the root tip. Secondary roots of sunflower seeds developed under the salt concentrations in the experiment were harvested within 24 to 72 h. After harvesting, the

roots were subjected to prefixation, fixation, hydrolysis and staining of biological materials required for microscopic analysis.

2.4. Microscopic Material Preparation

Salt-treated sunflower meristematic roots were harvested in the morning to capture the highest mitotic activity for 24 to 72 h. Fixation was conducted using Carnoy's reagent, obtained by preparing the solution in a 3:1 ratio of ethyl alcohol (96%) and glacial acetic acid [40,41]. Carnoy's reagent was added to the harvested biological material for 24 h at 2–4 degrees. Preservation of biological material for further studies was carried out at 2–4 degrees in 70% ethyl alcohol. The fixation solution was washed with 1N HCl at room temperature for 5 min. Hydrolysis was carried out with 2–3 mL of 1N HCI1 for 7–8 m in a water bath at 60 °C. The hydrolyzed solution was then finally removed with filter paper. Staining was carried out using Carr's reagents according to the Feulgen method [42], followed by the distribution of biological material using the squash method. The microscopic preparations obtained were analyzed under an Optika microscope at 400× magnification in normal light. Microscopic photographs were taken using the digital camera of the microscope. The data were then recorded and statistically processed.

2.5. Cytological and Statistical Analyses

Cytological studies were performed on a total of approximately 2500 cells from each treatment under each exposure time, and five microscopic fields of five individual roots were analyzed.

A cytogenetic study was conducted on meristematic tissues, differentiating between the effects of salt among the treatments according to the mitotic index. The mitotic index (MI) is the number of dividing cells relative to the number of cells in the microscopic field. During interphase, due to salt, an uneven distribution of chromatin leads to the appearance of atypical cells. During our studies, we encountered giant cells, abnormal cells and deformation of the nucleus, all of which we considered abnormal and were counted through the abnormal cell index (AC) (Figure 1). Analysis of genetic material during the cell cycle shows that provacuole formation occurs in prophase, after which provacuoles fuse to form the vacuole. In this situation, the evolution of chromosomes no longer follows a normal course, where they are instead distributed evenly or unevenly around the vacuole. This aspect led us to analyze the vacuolization index (IV) and prevacuolar index (CPI) under salt treatment. In meta-anaphase, when chromosomes become unichromatic by moving toward the poles of the cell, some asynchronous situations can be observed, leading to late (LC), sticky (SC) or irregular (IR) chromosomes, and sometimes creating chromosome bridges (CBs) or isolated chromosomes (ICs). All major indexes such as the mitotic index (MI), aberration index (CAI) and prevacuolar index (PVI) were compared with the vacuolization index (VI) to reflect the relationship between them under the effect of salt stress.

The calculation formulas used to determine the frequencies of the different chromosomal aberrations are as follows:

$$\mathbf{AC\%} = \frac{\mathbf{Nr.\ of\ cells\ with\ abnormal\ cells}}{\mathbf{Total\ number\ of\ cells}} \times \mathbf{100} \quad (1)$$

$$\mathbf{IRC\%} = \frac{\mathbf{Nr.\ of\ cells\ with\ irregularly\ chrom.}}{\mathbf{Total\ number\ of\ cells}} \times \mathbf{100} \quad (2)$$

$$\mathbf{CB\%} = \frac{\mathbf{Total\ number\ of\ bridge\ formation}}{\mathbf{Total\ number\ of\ cells}} \times \mathbf{100} \quad (3)$$

$$\mathbf{SC\%} = \frac{\mathbf{Total\ number\ with\ sticky\ chrom.}}{\mathbf{Total\ number\ of\ cells}} \times \mathbf{100} \quad (4)$$

$$\mathbf{IC\%} = \frac{\textbf{Total number of izolated chromosome}}{\textbf{Total number of cells}} \times \mathbf{100} \quad (5)$$

The equations used for the mitotic index (1), prophase index (2), metaphase index (3), anaphase index (4), telophase index (5), chromosomal aberration index (6), vacuolization index (7) and provacuolar index (8) are as follows:

$$\mathbf{MI\%} = \frac{\textbf{Number of cells in mitosis}}{\textbf{Total number of cells}} \times \mathbf{100} \quad (6)$$

$$\mathbf{Ip\%} = \frac{\textbf{Number of cells in prophase}}{\textbf{Total number of cells}} \times \mathbf{100} \quad (7)$$

$$\mathbf{Im\%} = \frac{\textbf{Number of cells in metaphase}}{\textbf{Total number of cells}} \times \mathbf{100} \quad (8)$$

$$\mathbf{Ia\%} = \frac{\textbf{Number of cells in anaphase}}{\textbf{Total number of cells}} \times \mathbf{100} \quad (9)$$

$$\mathbf{It\%} = \frac{\textbf{Number of cells in telopahse}}{\textbf{Total number of cells}} \times \mathbf{100} \quad (10)$$

$$\mathbf{CAI\%} = \frac{\textbf{Number of chromosomal aberation}}{\textbf{Total number of cells}} \times \mathbf{100} \quad (11)$$

$$\mathbf{VI\%} = \frac{\textbf{Number of vacuolized cells}}{\textbf{Total number of cells}} \times \mathbf{100} \quad (12)$$

$$\mathbf{PVI\%} = \frac{\textbf{Number of cells with provacuoles}}{\textbf{Total number of cells}} \times \mathbf{100} \quad (13)$$

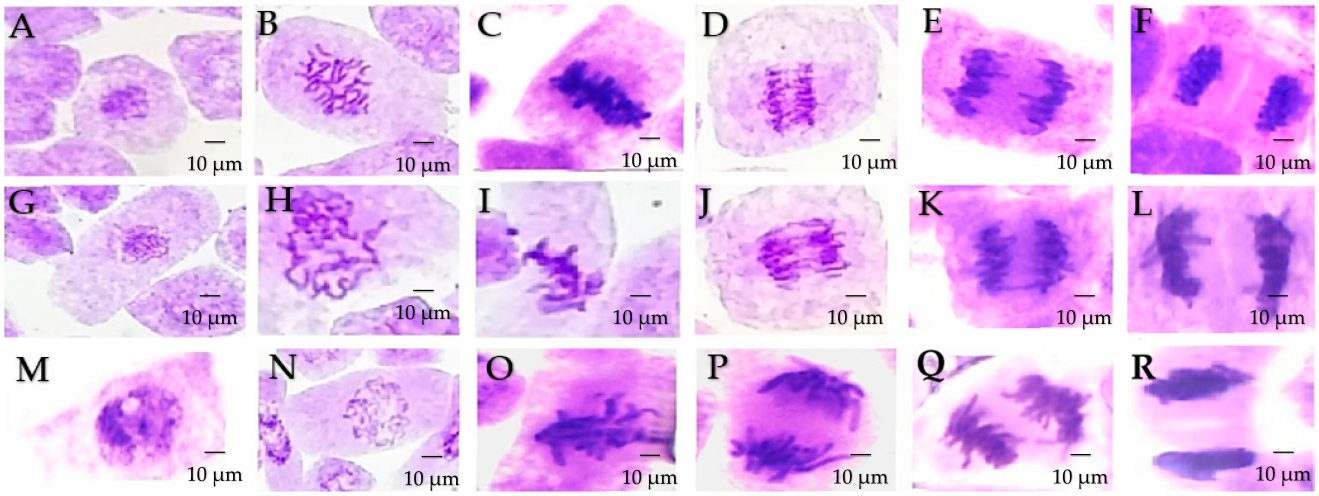

Figure 1. Control cellular division and abnormalities under NaCl stress: (**A**) Control prophase. (**B**) Karyotype of sunflower with 2n = 34 chromosomes. (**C**) Control metaphase. (**D**) Control anaphase. (**E**) Control anaphase. (**F**) Control telophase. (**G**) Giant cell (AC). (**H**) Irregularly moving chromosomes (IRC). (**I**) Disturbed metaphase (IRC). (**J**) Sticky chromosomes in anaphase (SC). (**K**) Chromosomal bridges in anaphase (CB). (**L**) Laggard chromosomes in telophase (LC). (**M**) Abnormal cells with visible nucleoli (AC). (**N**) Circular moving chromosomes (IRC). (**O**) Isolated chromosomes (IC). (**P**) Laggard chromosomes in anaphase (LC). (**Q**) Sticky chromosomes in anaphase (SC). (**R**) Asymmetric telophase (AC). (Magnification: 400×).

Data of the mean ± SE were subjected to one-way and two-way ANOVAs, with a significance level of $p < 0.05$. The comparison of different paired values among treatments and exposure times was carried out using the Tukey test. The statistical analysis was performed using the RStudio statistical package.

3. Results

3.1. Effect of Salt Stress on the Relationship between the Mitotic Index and Cell Vacuolization

The effect of different concentrations of salt used to examine mitotic activity showed a reduction in the number of dividing cells. The results showed a significant influence of the time of exposure to the saline solution and the concentration on the activity of mitotic divisions ($p > 0.001$) (Table 1).

Table 1. Analysis of variance of the combined effect of different salt concentrations and exposure times on the mitotic index.

Variance Source	DF *	SS *	Mean Sq	F Value	Pr (>F)
Treatment	3	3286	1380.3	405.54	2×10^{-16} ***
Exposure time	2	160	62.4	18.34	1.55×10^{-8} ***
Treatment × exposure time	6	18	6.8	1.984	0.0642
Residual	288	1205	4.2		

DF—degrees of freedom; SSsum of squares. The results were analyzed at significance levels of *** $p < 0.001$, ** $p < 0.01$ and * $p < 0.05$.

The highest mitotic index (MI) values were obtained in the salt-free treatment, obtaining 13.58%, 12.51% and 12.37% after 24, 48 and 72 h. On the other hand, at a concentration of 100 mM NaCl (V2), the mitotic index values were 9.95%, 8.20% and 7.30%. The lowest mitotic activity values were recorded at concentrations of 125 mM NaCl (V3), with 5.94%, 5.39% and 5.20%, plus 150 mM NaCl (V4), with 5.22%, 4.15% and 3.58%, over the 24–72 h exposure interval. Further analysis of the results of our studies revealed that the effect of salt stress also affected the percentage of other mitotic parameters (Table 2).

A decrease in the prophase index (Ip) was observed with increasing salt concentration, from 7% in the control samples to just over 1.5% in the samples treated with 150 mM NaCl. Other mitotic indices such as the metaphase index (Im), anaphase index (Ia) and telophase index (It) also decreased with increasing salt concentration and exposure time. When analyzed over a period of 24 to 72 h, the highest values for the NaCl solution treatments were observed at 24 h, while the lowest values were observed at 72 h ($p > 0.05$) (Table 2).

The results allow us to conclude that salt solutions cause stress in mitotic division and thus inhibit the growth and development of sunflower plants.

The vacuolization phenomenon develops when biological material is exposed to salt stress, but similarly, as the vacuolization index increases, the mitotic index decreases.

In our analysis, we observed that the mitotic index initially exceeded the vacuolization index in the control samples over all time intervals ($p > 0.05$) (Figure 2).

On the other hand, we observed a significant difference between the vacuolization index and the mitotic index during the first treatment with V2 saline, where the vacuolization index increased as the exposure duration increased, showing significant differences between the values in the 24–72 h interval ($p > 0.05$), which was not the case in the control samples. Inverse values proportional to the vacuolization phenomenon were evidenced by the decrease in the mitotic index in the 24–72 h time interval. As the salt concentration increased, the mitotic index decreased and the vacuolization index increased (Figure 2).

The vacuolization phenomenon is therefore closely linked to the decrease in the mitotic index and is a major factor in determining cell cytotoxicity.

Table 2. Results of mitotic activity under the influence of different salt treatments.

Variant	Time h	NaCl-mM	Total Number of Cells Analysed ± SE	Mitotic Index (%)	Prophase Index (%)	Metaphase Index (%)	Anaphase Index (%)	Telophase Index (%)
V1	24	0	2586 ± 2.58	**13.58 ± 0.5** ^{a}	7.04 ± 0.3 ^{a}	2.81 ± 0.23 ^{a}	2.1 ± 0.18 ^{ab}	1.62 ± 0.1 ^{a}
	48	0	2709 ± 2.11	**12.51 ± 0.52** ^{a}	5.36 ± 0.34 ^{bc}	3.04 ± 0.17 ^{a}	2.56 ± 0.14 ^{a}	1.54 ± 0.14 ^{a}
	72	0	2629 ± 1.50	**12.37 ± 0.46** ^{a}	5.96 ± 0.32 ^{ab}	2.4 ± 0.09 ^{ab}	2.29 ± 0.15 ^{a}	1.7 ± 0.07 ^{a}
V2	24	100	2597 ± 1.41	**9.95 ± 0.33** ^{b}	5.69 ± 0.18 ^{b}	1.93 ± 0.15 ^{bc}	1.54 ± 0.09 ^{bc}	0.78 ± 0.09 ^{b}
	48	100	2707 ± 1.73	**8.2 ± 0.4** ^{bc}	5.08 ± 0.23 ^{bcd}	1.53 ± 0.14 ^{cd}	1.11 ± 0.07 ^{cd}	0.46 ± 0.09 ^{b}
	72	100	2540 ± 2.17	**7.3 ± 0.47** ^{cd}	3.88 ± 0.29 ^{de}	1.53 ± 0.09 ^{cd}	1.29 ± 0.08 ^{cd}	0.58 ± 0.09 ^{b}
V3	24	125	2787 ± 2.08	**5.94 ± 0.41** ^{de}	4.32 ± 0.25 ^{cd}	0.94 ± 0.06 ^{d}	0.31 ± 0.09 ^{e}	0.35 ± 0.09 ^{b}
	48	125	2742 ± 2.54	**5.2 ± 0.44** ^{ef}	2.98 ± 0.27 ^{ef}	0.92 ± 0.02 ^{d}	0.72 ± 0.13 ^{de}	0.56 ± 0.09 ^{b}
	72	125	2630 ± 2.43	**4.62 ± 0.24** ^{ef}	2.81 ± 0.24 ^{ef}	0.96 ± 0.02 ^{d}	0.32 ± 0.13 ^{e}	0.52 ± 0.12 ^{b}
V4	24	150	2701 ± 2.30	**5.22 ± 0.22** ^{def}	2.64 ± 0.14 ^{efg}	1.27 ± 0.15 ^{cd}	0.71 ± 0.08 ^{de}	0.59 ± 0.08 ^{b}
	48	150	2727 ± 1.97	**4.15 ± 0.26** ^{ef}	2.16 ± 0.16 ^{fg}	0.94 ± 0.16 ^{d}	0.47 ± 0.09 ^{e}	0.57 ± 0.09 ^{b}
	72	150	2602 ± 1.85	**3.58 ± 0.38** ^{f}	1.6 ± 0.16 ^{g}	1.18 ± 0.19 ^{d}	0.46 ± 0.09 ^{e}	0.31 ± 0.09 ^{b}

Superscript letters are used according to the results of the Tukey pairwise comparison test and represent the significance levels of each column value obtained as a function of the NaCl concentration and exposure time. The highest values are noted, starting with the first letter "a". The similarity between the superscript letters reflects non-significant differences between the values obtained ($p > 0.05$).

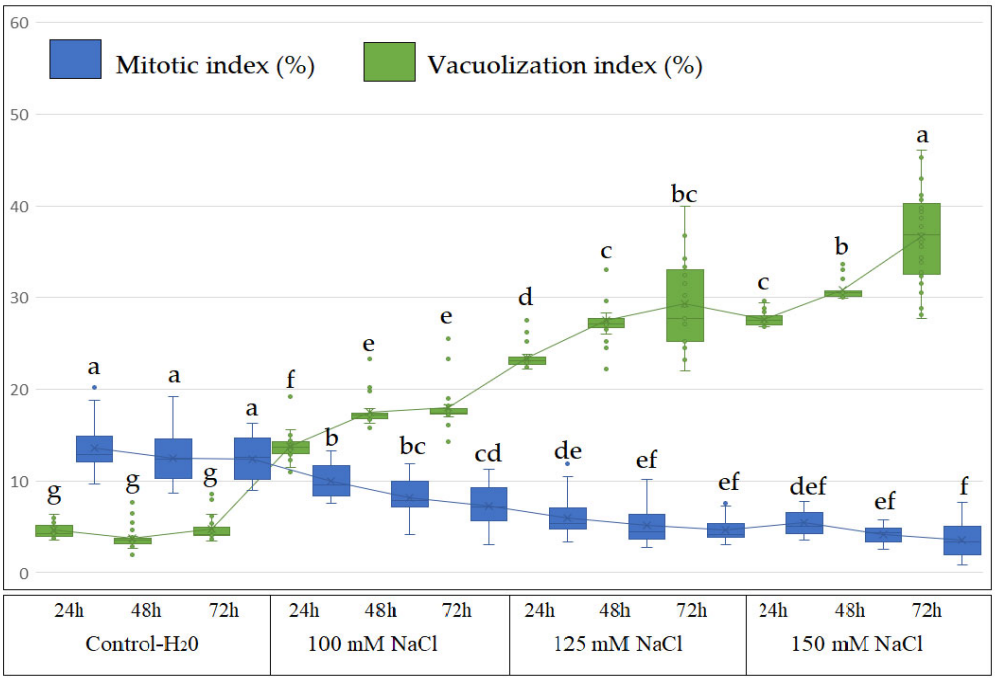

Figure 2. Boxplot representation of the mitotic index and vacuolization index as a function of different salt concentrations for 24 h–72 h exposure times. Superscript letters are used according to the results of the Tukey pairwise comparison test and represent the significance levels of each column value obtained as a function of the NaCl concentration and exposure time. The highest values are noted, starting with the first letter "a". The similarity between the superscript letters reflects non-significant differences between the values obtained ($p > 0.05$).

3.2. Effect of Salt Stress on the Relationship between the Chromosomal Aberration Index and Cell Vacuolization

Regarding the effect of salt stress on the chromosomal aberration index, a significant increase was observed with increasing salt exposure interval and concentration, and with the combined effect of both ($p > 0.001$) (Table 3).

Table 3. Analysis of variance of the combined effect of different salt concentrations and exposure times on the chromosomal aberration index.

Variance Source	DF *	SS *	Mean Sq	F Value	Pr (>F)
Treatment	3	3799	1266.5	249.088	2×10^{-16} ***
Exposure time	2	418	208.9	41.087	2×10^{-13} ***
Treatment × exposure time	6	156	26.0	5.117	5.16×10^{-5} ***
Residual	288	1464	5.1		

DF—degrees of freedom; SS—sum of squares. The results were analyzed at significance levels of *** $p < 0.001$, ** $p < 0.01$ and * $p < 0.05$.

The chromosomal aberration index (CAI) increased with the increase in the salt concentration, where, at an exposure time of 24 h, we obtained percentage values of 0.96% in V1, 2.39% in V2, 5.35% in V3 and 7.93% in V4. The difference between the values in the 24–72 h time interval for each salt concentration showed an increase in the number of chromosomal aberrations, obtaining a maximum value of 11.82 at the highest concentration and exposure time analyzed. Analysis of the frequency of chromosomal aberrations between the non-salt-treated samples (V1) and salt-treated samples (V2, V3 and V4) revealed a significant increase ($p < 0.05$). There was an increase in the number of irregularly moving chromosomes (IRCs), an increase in the number of sticky chromosomes, and an increase in the number of lagging chromosomes, as well as a moderate increase in the number of

isolated chromosomes. In the case of chromosomal bridge (CB) formation, there was an increase in the percentage under salt stress.

In the control samples, the percentage of chromosomal aberrations was the lowest, with only irregular chromosome movements and abnormal-type aberrations present, together accounting for less than 1% of ICAs, with the other types of chromosomal aberrations being absent in the salt-free treatment (V1). The results showed that the number of chromosomal aberration types began to increase as the salt concentration used increased (Table 3).

The percentage of chromosomal aberrations of irregular chromosome movement (IRCs) ranged from less than 1% in samples without saline to more than 5% in those with higher saline concentrations ($p < 0.05$). In the V4 treatment, irregular chromosome movement (IRCs) was more prominent, characterized by circular chromosome movements, which may be associated with division block. The cytotoxic effect of the high salt concentrations was also reflected in the high percentage of lagging chromosomes. This type of chromosomal aberration did not occur in the control samples but was present in 2% of the 150 mM NaCl salt samples (V4). Another chromosomal anomaly caused by the cytotoxic effect of salt is determined by the appearance of isolated chromosomes. These did not appear in the samples without salt, and even at 100 mM, their percentage was very low. The higher salt concentrations of 125 mM (V3) and 150 mM (V4) induced a significant percentage of isolated chromosomes compared with the control samples ($p < 0.05$), where, at 125 mM and 150 mM, the percentage values were close to 1%. The frequency of chromosome bridge formation was also increased by the salt exposure time. The highest values were recorded at a NaCl concentration of 150 mM, with the frequency decreasing at lower salt concentrations and being absent in the control samples containing only water (Table 4).

The increase in the percentage of chromosomal aberrations is directly proportional to the salt concentration and exposure time. Thus, the cytotoxicity of salt is evidenced by the presence of chromosomal aberrations that ultimately block the normal progression of the division spindle, leading to plant growth inhibition (Figure 3).

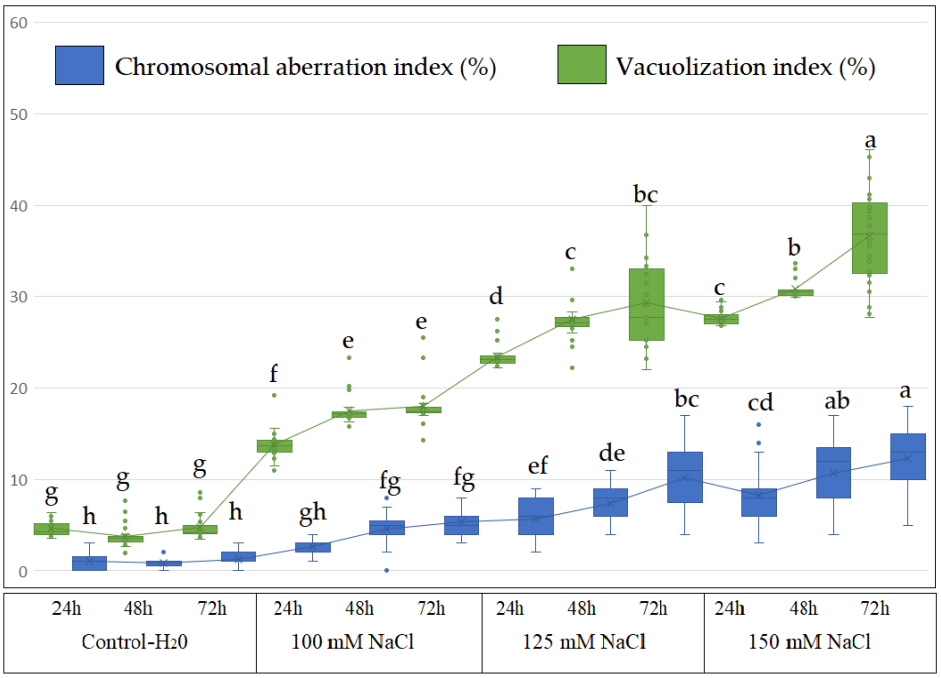

Figure 3. Boxplot representation of the chromosomal aberration index and vacuolization index as a function of different salt concentrations for 24 h–72 h exposure times. Superscript letters are used according to the results of the Tukey pairwise comparison test and represent the significance levels of each column value obtained as a function of the NaCl concentration and exposure time. The highest values are noted, starting with the first letter "a". The similarity between the superscript letters reflects non-significant differences between the values obtained ($p > 0.05$).

Table 4. Results concerning the effect of salt on the chromosomal aberration index and the frequency of different types of abnormalities during mitotic division.

Variant	Time (h)	NaCl-mM	Total Number of Aberant Cells	Chromosomal Aberration Index (CAI) (%)	Abnormal Cells (AC) (%)	Irregular Movement of the Chromosome (IRC) (%)	Chromosomes Bridges (CB) (%)	Sticky Chromosomes (SC) (%)	Isolated Chromosomes (IC) (%)	Lagging Chromosomes (LC) (%)
V1	24	0	25 ± 0.17	**0.96 ± 0.17 ^{h}**	0.19 ± 0.08 ^{c}	0.77 ± 0.16 ^{f}	-	-	-	-
	48	0	20 ± 0.09	**0.73 ± 0.09 ^{h}**	0.29 ± 0.09 ^{c}	0.44 ± 0.12 ^{f}	-	-	-	-
	72	0	30 ± 0.16	**1.14 ± 0.16 ^{h}**	0.49 ± 0.16 ^{bc}	0.64 ± 0.14 ^{f}	-	-	-	-
V2	24	100	65 ± 0.12	**2.39 ± 0.12 ^{gh}**	0.33 ± 0.09 ^{bc}	0.99 ± 0.22 ^{f}	0.36 ± 0.12 ^{de}	0.51 ± 0.12 ^{cd}	-	0.18 ± 0.08 ^{de}
	48	100	115 ± 0.32	**4.52 ± 0.32 ^{fg}**	0.86 ± 0.19 ^{abc}	1.61 ± 0.26 ^{ef}	0.62 ± 0.15 ^{cde}	0.7 ± 0.18 ^{bcd}	0.35 ± 0.13 ^{def}	0.35 ± 0.09 ^{de}
	72	100	134 ± 0.25	**4.96 ± 0.25 ^{fg}**	1.25 ± 0.21 ^{a}	1.44 ± 0.19 ^{ef}	0.77 ± 0.16 ^{bcd}	0.77 ± 0.17 ^{bc}	0.4 ± 0.15 ^{cdef}	0.29 ± 0.13 ^{de}
V3	24	125	141 ± 0.43	**5.36 ± 0.43 ^{ef}**	0.79 ± 0.16 ^{abc}	2.32 ± 0.2 ^{de}	0.57 ± 0.18 ^{cde}	0.95 ± 0.22 ^{abc}	0.22 ± 0.08 ^{ef}	0.49 ± 0.11 ^{cde}
	48	125	185 ± 0.37	**6.63 ± 0.37 ^{de}**	0.89 ± 0.2 ^{abc}	2.61 ± 0.3 ^{cd}	0.71 ± 0.16 ^{bcd}	0.96 ± 0.16 ^{abc}	0.43 ± 0.13 ^{cdef}	1 ± 0.11 ^{bc}
	72	125	254 ± 0.65	**9.31 ± 0.65 ^{bc}**	1.46 ± 0.12 ^{a}	3.48 ± 0.3 ^{abc}	0.73 ± 0.19 bcd	1.13 ± 0.18 ^{abc}	1.24 ± 0.17 ^{ab}	1.24 ± 0.15 ^{ab}
V4	24	150	206 ± 0.62	**7.93 ± 0.62 ^{cd}**	0.88 ± 0.19 ^{abc}	3.15 ± 0.21 ^{bcd}	1.19 ± 0.17 ^{abc}	1.15 ± 0.18 ^{abc}	0.8 ± 0.17 ^{bcd}	0.73 ± 0.16 ^{bcd}
	48	150	267 ± 0.66	**9.73 ± 0.66 ^{ab}**	1.05 ± 0.23 ^{ab}	3.82 ± 0.27 ^{ab}	1.34 ± 0.31 ^{ab}	1.23 ± 0.21 ^{ab}	0.94 ± 0.17 ^{abc}	1.31 ± 0.31 ^{ab}
	72	150	308 ± 0.7	**11.83 ± 0.7 ^{a}**	1.3 ± 0.19 ^{a}	4.41 ± 0.37 ^{a}	1.69 ± 0.18 ^{a}	1.46 ± 0.24 ^{a}	1.38 ± 0.15 ^{a}	1.57 ± 0.21 ^{a}

Superscript letters are used according to the results of the Tukey pairwise comparison test and represent the significance levels of each column value obtained as a function of the NaCl concentration and exposure time. The highest values are noted, starting with the first letter "a". The similarity between the superscript letters reflects non-significant differences between the values obtained ($p > 0.05$).

From our comparative analyses, the vacuolization index and chromosomal aberration index showed significantly different values between the treated samples and the control samples in the 24–72-h time interval (Figure 3).

On the other hand, the increase in the percentage of chromosomal aberrations was also accompanied by an increase in the vacuolization index, both increasing with the salt concentration and time interval. Thus, we can say that there is a close link between the increases in the vacuolization index and chromosomal aberration index, where cell vacuolization represents the maximum cytotoxic effect, since the vacuolized cell can no longer maintain the formation of the cell division spindle. This is sometimes evidenced by the circular movements of other chromosomes and the consequent inhibition of plant development.

3.3. Effect of Salt Stress on the Relationship between Cell Vacuolization and the Provacuolar Index

The increase in the vacuolization index was influenced by both the concentration of saline used and the exposure time, with a high degree of significance ($p < 0.001$). The combined effect of the treatment and exposure time showed an increase in the vacuolization index. Thus, we can say that the vacuolization phenomenon is closely related to the cytotoxicity caused by the saline solutions used. Vacuolized cells are formed by the fusion of provacuoles in response to salt stress. The number of cells with multiple provacuoles increased considerably with increasing saline concentrations ($p < 0.001$) (Table 5).

Table 5. Analysis of variance of the combined effect of different salt concentrations and exposure times on the vacuolization and provacuolar indices.

Vacuolization Index (VI)					
Variance Source	**DF ***	**SS ***	**Mean Sq**	**F Value**	**Pr (>F)**
Treatment	3	37544	12515	2092.87	2×10^{-16} ***
Exposure time	2	1396	698	116.73	2×10^{-16} ***
Treatment × exposure time	6	640	107	17.84	5.16×10^{-5} ***
Residual	288	1722	6		
Provacuolar Index (PVI)					
Variance Source	**DF ***	**SS ***	**Mean Sq**	**F Value**	**Pr (>F)**
Treatment	3	1307.1	435.7	184.728	2×10^{-16} ***
Exposure time	2	7.1	3.5	1.502	0.2244
Treatment × exposure time	6	44.2	7.4	3.121	0.0056 **
Residual	288	679.3	2.4		

DF—degrees of freedom; SS—sum of squares. The results were analyzed at significance levels of *** $p < 0.001$, ** $p < 0.01$ and * $p < 0.05$.

Another important effect of salt toxicity is the increase in the provacuolar index (PVI). At the cellular level, under the influence of salt stress, a cytological process is observed consisting in the formation of provacuoles, which fuse to form an enlarged vacuole in which the genetic material is arranged around it. The vacuolization phenomenon develops when the biological material is exposed to salt stress with an increasing frequency as a function of the NaCl concentration.

The vacuolization phenomenon showed an increasing frequency concomitant with the duration of exposure to the salt solutions, whereby for the 24-h exposure duration we recorded the lowest values for the salt concentrations, while the highest values were recorded for the 72-h exposure duration, culminating in a maximum value of more than 36% of cells vacuolized under a salt concentration of 150 mM (Table 6). Therefore, a correlation was found between the increases in the provacuolar index and vacuolization index ($p < 0.05$).

Table 6. Results of the effect of salt on the vacuolization index and provacuolar index.

Variant	Time	Treatment	Total Number of Cells Analysed ± SE	Vacuolization Index (VI)	Provacuolar Index (PVI)
V1	24	0	2586 ± 2.58	**4.61 ± 0.17 ^{g}**	**2.5 ± 0.25 ^{f}**
	48	0	2709 ± 2.11	**3.75 ± 0.23 ^{g}**	**2.56 ± 0.23 ^{f}**
	72	0	2629 ± 1.50	**4.74 ± 0.25 ^{g}**	**2.54 ± 0.23 ^{f}**
V2	24	100	2597 ± 1.41	**13.75 ± 0.3 ^{f}**	**4.97 ± 0.31 ^{e}**
	48	100	2707 ± 1.73	**17.52 ± 0.29 ^{e}**	**5.87 ± 0.36 ^{de}**
	72	100	2540 ± 2.17	**17.98 ± 0.41 ^{e}**	**5.14 ± 0.3 ^{e}**
V3	24	125	2787 ± 2.08	**23.41 ± 0.23 ^{d}**	**6.92 ± 0.29 ^{bcd}**
	48	125	2742 ± 2.54	**27.56 ± 0.49 ^{c}**	**5.82 ± 0.27 ^{de}**
	72	125	2630 ± 2.43	**29.28 ± 0.94 ^{bc}**	**6.22 ± 0.3 ^{bcde}**
V4	24	150	2701 ± 2.30	**27.66 ± 0.17 ^{c}**	**7.45 ± 0.31 ^{b}**
	48	150	2727 ± 1.97	**30.81 ± 0.19 ^{b}**	**7.33 ± 0.35 ^{bc}**
	72	150	2602 ± 1.85	**36.62 ± 1 ^{a}**	**9.05 ± 0.41 ^{a}**

Superscript letters are used according to the results of the Tukey pairwise comparison test and represent the significance levels of each column value obtained as a function of the NaCl concentration and exposure time. The highest values are noted, starting with the first letter "a". The similarity between the superscript letters reflects non-significant differences between the values obtained ($p > 0.05$).

Cell vacuolization occurs under stress conditions of different salt concentrations. Vacuolized cells show a distribution of genetic material around the vacuole, and the tonoplast of the vacuole is well defined. Vacuolization is a very important topic in salt stress determination, which has applications in the selection of salt-stress-resistant genotypes in plant research and development programs. Vacuolization also plays a role in the diagnosis of cell stress, as the vacuolization index is significantly higher in salt treatments than in salt-free treatments ($p < 0.05$). Therefore, we can identify how at a physiological level, cells are stressed due to salinity or other stressors in both human and plant cells.

The effect of salt stress was also observed in our analyses based on the appearance of cell vacuolization. According to our studies, we observed an increase in the rate of cells with provacuoles, ranging from two to seven provacuoles in some cases (Figure 4B). The provacuoles fused (Figure 4AC), forming an enlarged vacuole with genetic material arranged around it (Figure 4F). The increase in the provacuolar index was due to the higher salt concentrations. Thus, we can conclude that high concentrations of NaCl accumulate in the vacuoles of cells. Circular movement of the chromosomes was observed in the vacuolized cells (Figure 4D).

From our results (Figure 5), no changes in the provacuolar and vacuolization indices were identified in the control samples. On the other hand, the increase in the provacuolar index with the vacuolization index was directly proportional to the NaCl concentration and exposure time.

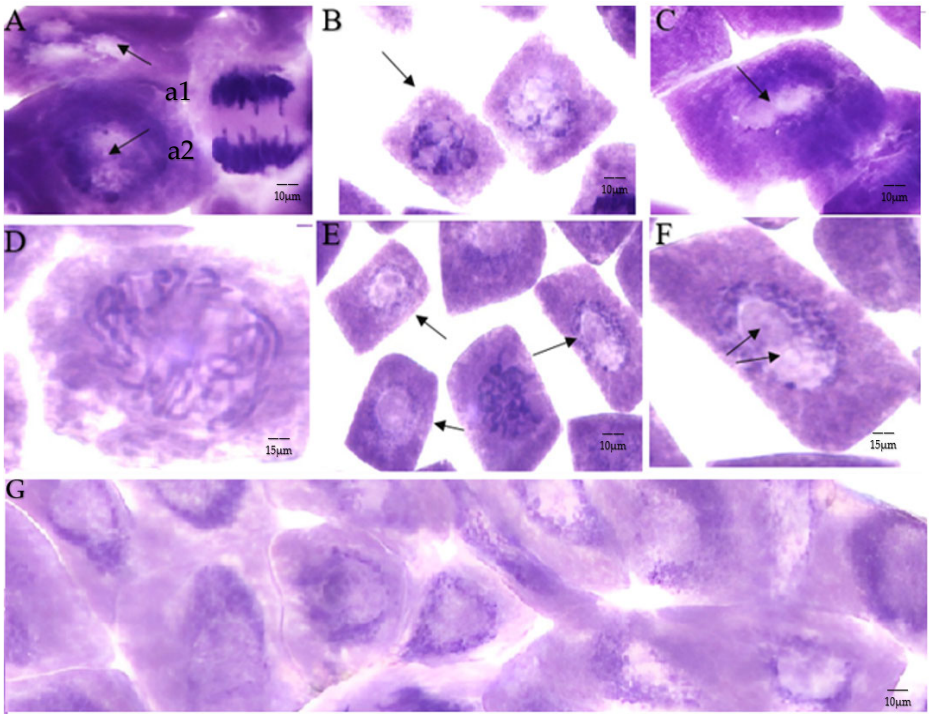

Figure 4. Vacuolized cell formation: cells with multiple provacuoles (**A**, a1), fusion of provacuoles (**A**, a2); cells with multiple provacuoles (**B**); fusion of provacuoles (**C**); circular movement of the chromosomes in metaphase (**D**); normal metaphase with vacuolized cells around it (**E**); presence of nucleoli in the vacuolized cells (**F**); vacuolized cells under 150 mM of NaCl at the 72 h exposure time (**G**) (magnification: 400×).

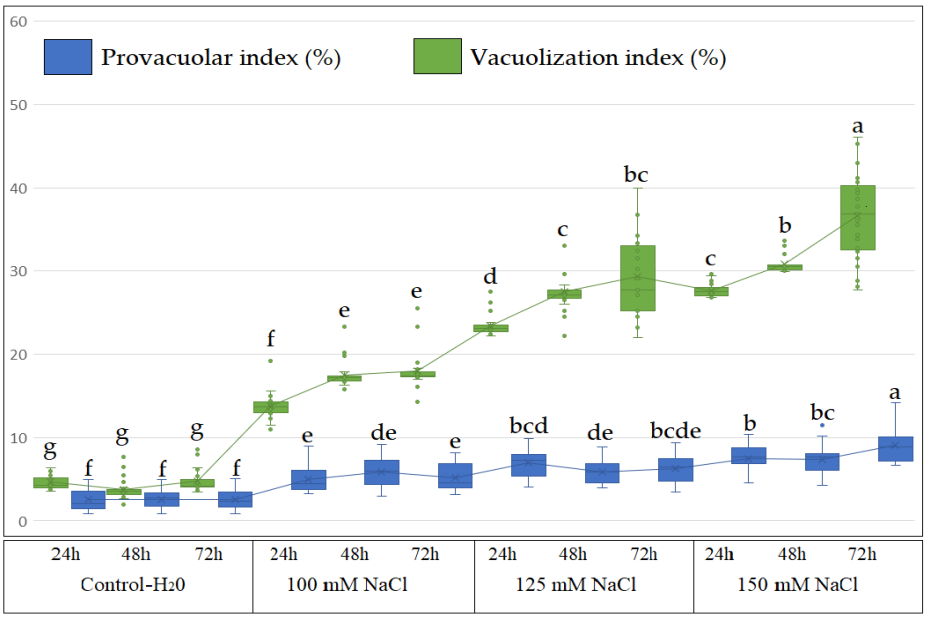

Figure 5. Boxplot representation of the provacuolar index and vacuolization index as a function of different salt concentrations for 24 h–72 h exposure times. Superscript letters are used according to the results of the Tukey pairwise comparison test and represent the significance levels of each column value obtained as a function of the NaCl concentration and exposure time. The highest values are noted, starting with the first letter "a". The similarity between the superscript letters reflects non-significant differences between the values obtained ($p > 0.05$).

4. Discussion

According to the results obtained, the vacuolization phenomenon was observed as early as the first treatment with 100 mM NaCl (V2). The rapid and significant accumulation of NaCl in the plant cell leads to the induction and formation of provacuoles, the main factor in vacuole formation [43]. The longer the exposure time and the higher the salt concentration, the more evident the vacuolization phenomenon. Furthermore, the results showed a significant increase in the provacuolar index (PVI), synchronized with the increase in the vacuolization index (VI). This marked increase in the provacuolar index and vacuolization index is due to the accumulation of salt in the vacuole, which also deregulates normal osmotic processes [44] and cell division by decreasing the mitotic index. Reversible vacuoles in *Helianthus annuus* cells show normal activity under control treatments, as they are in continuous homeostatic equilibrium motion [45].

Vacuolization is also known to improve cell survival by reducing stress [23]. With the increase in the vacuolization index, normally dividing cells were found to be surrounded by vacuolized cells responsible for salt accumulation in vacuoles, highlighting the adaptive role of vacuolization in the plant tolerance mechanism. This can be seen in Figure 4D, where a circular movement of the chromosomes is observed in the vacuolized cells. Conversely, in Figure 4E, we see a normal metaphase surrounded by vacuolized cells, which reflects the importance of vacuolization in the adaptive process by accumulating NaCl in the cells and sustaining the normal mitotic division by reducing the salt concentration around it.

On the other hand, our results indicate that the increase in the vacuolization index (VI) is inversely proportional to the mitotic index (MI). Studies have indicated the cellular mechanism of the effect of salt stress on plants [46]. The negative influence of salt stress on mitotic division was observed at the cellular level, with the cell division spindle blocked by circularly moving chromosomes (Figure 4D).

Studies on *Oryza sativa* indicate that vacuole destruction correlates with programmed cell death (PCD) [47]. The correlation between time and the level of exposure to different salt concentrations resulted in a synchronized response with an increase in the vacuolization index and a decrease in the mitotic index, highlighting the close link between them. A close link between vacuolization and chromosomal aberrations has also been observed. Research indicates that the vacuolization phenomenon is influenced by the endoplasmic reticulum in the sunflower, where the presence of salt stress tolerance expression genes is also localized [48].

The increase in the chromosomal aberration index at different NaCl concentrations recorded in our studies has been confirmed by numerous cytological investigations carried out on plant tissues [49–51]. The effect of salt can also be seen in the investigation carried out by Affenzeller et al. (2009) [52] on the percentage of cell viability in Micrasterias denticulate after treatment with 200 mM NaCl, where they observed that after 6 h of exposure, around 80% of the cells were viable, but after 48 h of NaCl exposure, cell viability decreased to 40%. Morphological changes were observed in cell organelles: after 24 h of NaCl treatment, there was an increase in the number of mitochondria, disintegration of the Golgi apparatus into numerous small vesicles with swelling and dilatation of endoplasmic reticulum compartments, highlighting the effect of salt on the appearance of autophagy during programmed cell death (PCD) [53,54]. The same phenomenon has been found in the results of H_2O_2 exposure inducing PCD in cells [55,56].

Studies show that PCD is accompanied by tonoplast cleavage (vacuole collapse) and leakage of vacuole contents into the cytoplasm. Thus, hydrolytic enzymes present in the vacuole reach the cytoplasm and begin organelle degradation, i.e., the start of the PCD process [57]. Research indicates that class I NHX antiporters are present in the tonoplast and play a role in Na^+/H^+ exchange. NHX antiporters are active at high NaCl concentrations. Antiporters enhance and protect cells from the effect of salt stress [58,59]. Research also confirms the phenomenon of vacuolization and the fusion of provacuoles into large vacuoles located in the center of the cell under the effect of salt stress [60–62]. Moreover, research has reported a correlation between the effect of NaCl stress and the

appearance of vacuolization and PCD as an effect of ionic imbalances present in salt treatments in *Arabidopsis* [63]. Cell vacuolization occurs not only under salt stress, but also under heavy-metal stress [64–66]. The vacuolization phenomenon occurs not only in plant cells but also in cancerous tissue [67,68] and other liver cell diseases [69,70].

Consequently, the vacuolization phenomenon can be a very useful cytological diagnostic method both for selecting and developing valuable genotypes, and for diagnosing diseases and prescribing treatments by reducing the vacuolization index (VI) and thus helping to protect cell life.

5. Conclusions and Future Perspectives

The cytological analyses showed a decrease in the mitotic index and an increase in the number of chromosomal aberrations in the presence of salt solutions. The decrease in the mitotic index (MI) and the increase in the number of chromosomal aberrations were more prominent when the salt stress exposure duration increased and the salt solution concentration was higher. Another cytological response caused by salt stress was an increase in the provacuolar index (PVI). Provacuoles fuse into irreversible vacuoles and induce the disposition of genetic material around them. The increase in the vacuolization index (VI) was directly proportional to the increases in the time of exposure to NaCl and the concentration levels.

We can conclude that salt stress causes vacuolization of sunflower cells, a decrease in the mitotic index and an increase in the number of chromosomal abnormalities, inhibiting the growth and development of plants. Our future studies will monitor the development of sunflower genotypes tolerant to salt stress in our breeding programs by tracking the vacuolization index. In the future, we will also analyze the phenomenon of vacuolization as a function of soil acidity and its influence on the development of sunflower plants.

Author Contributions: The authors have contributed to the work as follows: O.E., S.I. and P.I., analysis and interpretation of data obtained; S.I., preparation of biological material for analysis; O.E., S.I., P.I. and S.C., cytological analysis and interpretation of vacuolization phenomenon; O.E. and P.I., study and literature consultation on vacuolization phenomenon; P.I., microscopic imaging; S.C., anatomical study of sunflower cells; O.E., applied interpretation of vacuolization phenomenon in sunflower breeding programs; S.I., P.I., S.C., C.A., C.D. and P.R., review and validation of the article. All authors have read and agreed to the published version of the manuscript.

Funding: This research paper was supported by the project "Increasing the impact of excellence research on the capacity for innovation and technology transfer within USAMVB Timișoara", code 6PFE, submitted to the competition Program 1—Development of the national system of research-development, Subprogram 1.2—Institutional performance, Institutional development projects—Development projects of excellence in RDI.

Institutional Review Board Statement: The research conducted in this article did not involve animals or humans.

Informed Consent Statement: Not applicable.

Data Availability Statement: Data are contained within the article.

Acknowledgments: The authors would like to thank the funding institutions.

Conflicts of Interest: The authors declare no conflict of interest.

References

1. Bybordi, A. The Influence of Salt Stress on Seed Germination, Growth and Yield of Canola Cultivars. *Not. Bot. Horti Agrobot. Cluj-Napoca* **2010**, *38*, 128–133. [CrossRef]
2. Cokkizgin, A. Salinity Stress in Common Bean (*Phaseolus vulgaris* L.) Seed Germination. *Not. Bot. Horti Agrobot. Cluj-Napoca* **2012**, *40*, 177–182. [CrossRef]
3. Duca, M.; Boian, I.; Domenco, R. The impact of droughts on sunflower production in the Republic of Moldova. *Not. Bot. Horti Agrobot. Cluj-Napoca* **2022**, *50*, 13040. [CrossRef]

4. Mu, Y.; Lin, J.; Mu, C.; Gao, Z. Effects of NaCl Stress on the Growth and Physiological Changes in Oat (*Avena sativa*) Seedlings. *Not. Bot. Horti Agrobot. Cluj-Napoca* **2015**, *43*, 468–472. [CrossRef]
5. El-Taher, A.M.; El-Raouf, H.S.A.; Osman, N.A.; Azoz, S.N.; Omar, M.A.; Elkelish, A.; El-Hady, M.A.M.A. Effect of Salt Stress and Foliar Application of Salicylic Acid on Morphological, Biochemical, Anatomical, and Productivity Characteristics of Cowpea (*Vigna unguiculata* L.) Plants. *Plants* **2021**, *11*, 115. [CrossRef]
6. Liu, L.; Wang, B. Protection of Halophytes and Their Uses for Cultivation of Saline-Alkali Soil in China. *Biology* **2021**, *10*, 353. [CrossRef]
7. AL Hassan, M.; Fuertes, M.M.; Sánchez, F.J.R.; Vicente, O.; Boscaiu, M. Effects of Salt and Water Stress on Plant Growth and on Accumulation of Osmolytes and Antioxidant Compounds in Cherry Tomato. *Not. Bot. Horti Agrobot. Cluj-Napoca* **2015**, *43*, 1–11. [CrossRef]
8. Marakli, S.; Temel, A.; Gozukirmizi, N. Salt Stress and Homobrassinosteroid Interactions during Germination in Barley Roots. *Not. Bot. Horti Agrobot. Cluj-Napoca* **2014**, *42*, 446–452. [CrossRef]
9. Tabur, S.; Demir, K. Role of some growth regulators on cytogenetic activity of barley under salt stress. *Plant Growth Regul.* **2010**, *60*, 99–104. [CrossRef]
10. Tilkat, E.A.; Haşimi, N.; Kuru, I.S.; Süzerer, V. Antioxidant and antimicrobial responses associated with in vitro salt stress of in vitro and in vivo grown Pistacia khinjuk stocks. *Not. Bot. Horti Agrobot. Cluj-Napoca* **2020**, *48*, 1885–1900. [CrossRef]
11. Jabeen, N.; Ahmad, R. Foliar Application of Potassium Nitrate Affects the Growth and Nitrate Reductase Activity in Sunflower and Safflower Leaves under Salinity. *Not. Bot. Horti Agrobot. Cluj-Napoca* **2011**, *39*, 172. [CrossRef]
12. Jalal, R.S.; Abulfaraj, A.A. Exogenous application of agmatine improves water stress and salinity stress tolerance in turnip (*Brassica rapa* L.). *Not. Bot. Horti Agrobot. Cluj-Napoca* **2022**, *50*, 12601. [CrossRef]
13. Ahanger, M.A.; Tomar, N.S.; Tittal, M.; Argal, S.; Agarwal, R.M. Plant growth under water/salt stress: ROS production; antioxidants and significance of added potassium under such conditions. *Physiol. Mol. Biol. Plants* **2017**, *23*, 731–744. [CrossRef]
14. Liu, J.; Fu, C.; Li, G.; Khan, M.N.; Wu, H. ROS Homeostasis and Plant Salt Tolerance: Plant Nanobiotechnology Updates. *Sustainability* **2021**, *13*, 3552. [CrossRef]
15. Zhang, M.; Smith, J.A.C.; Harberd, N.P.; Jiang, C. The regulatory roles of ethylene and reactive oxygen species (ROS) in plant salt stress responses. *Plant Mol. Biol.* **2016**, *91*, 651–659. [CrossRef]
16. Jha, Y.; Subramanian, R.B. PGPR regulate caspase-like activity, programmed cell death, and antioxidant enzyme activity in paddy under salinity. *Physiol. Mol. Biol. Plants* **2014**, *20*, 201–207. [CrossRef]
17. Petrov, V.; Hille, J.; Mueller-Roeber, B.; Gechev, T.S. ROS-mediated abiotic stress-induced programmed cell death in plants. *Front. Plant Sci.* **2015**, *6*, 69. [CrossRef] [PubMed]
18. Purcarea, C.; Laslo, V.; Memete, A.R.; Agud, E.; Miere, F.; Vicas, S.I. Antigenotoxic and Antimutagenic Potentials of Proline in *Allium cepa* Exposed to the Toxicity of Cadmium. *Agriculture* **2022**, *12*, 1568. [CrossRef]
19. Fahad, S.; Hussain, S.; Matloob, A.; Khan, F.A.; Khaliq, A.; Saud, S.; Hassan, S.; Shan, D.; Khan, F.; Ullah, N.; et al. Phytohormones and plant responses to salinity stress: A review. *Plant Growth Regul.* **2014**, *75*, 391–404. [CrossRef]
20. Fahad, S.; Hussain, S.; Bano, A.; Saud, S.; Hassan, S.; Shan, D.; Khan, F.A.; Khan, F.; Chen, Y.; Wu, C.; et al. Potential role of phytohormones and plant growth-promoting rhizobacteria in abiotic stresses: Consequences for changing environment. *Environ. Sci. Pollut. Res.* **2014**, *22*, 4907–4921. [CrossRef]
21. Dubois, E.; Scherens, B.; Vierendeels, F.; Ho, M.M.W.; Messenguy, F.; Shears, S.B. In Saccharomyces cerevisiae, the Inositol Polyphosphate Kinase Activity of Kcs1p Is Required for Resistance to Salt Stress, Cell Wall Integrity, and Vacuolar Morphogenesis. *J. Biol. Chem.* **2002**, *277*, 23755–23763. [CrossRef] [PubMed]
22. Silva, P.; Gerós, H. Regulation by salt of vacuolar H^+-ATPase and H^+-pyrophosphatase activities and Na^+/H^+ exchange. *Plant Signal. Behav.* **2009**, *4*, 718–726. [CrossRef] [PubMed]
23. Shubin, A.V.; Demidyuk, I.V.; Komissarov, A.A.; Rafieva, L.M.; Kostrov, S.V. Cytoplasmic vacuolization in cell death and survival. *Oncotarget* **2016**, *7*, 55863–55889. [CrossRef]
24. Hussain, M.; Ahmad, S.; Hussain, S.; Lal, R.; Ul-Allah, S.; Nawaz, A. Rice in Saline Soils: Physiology, Biochemistry, Genetics, and Management. *Adv. Agron.* **2018**, *148*, 231–287. [CrossRef]
25. Carillo, P.; Annunziata, M.G.; Pontecorvo, G.; Fuggi, A.; Woodrow, P. Salinity stress and salt tolerance. *Abiotic Stress Plants-Mech. Adapt.* **2011**, *1*, 21–38.
26. Alkhatib, R.; Abdo, N.; Mheidat, M. Photosynthetic and Ultrastructural Properties of Eggplant (*Solanum melongena*) under Salinity Stress. *Horticulturae* **2021**, *7*, 181. [CrossRef]
27. Duan, W.; Lu, B.; Liu, L.; Meng, Y.; Ma, X.; Li, J.; Zhang, K.; Sun, H.; Zhang, Y.; Dong, H.; et al. Effects of Exogenous Melatonin on Root Physiology, Transcriptome and Metabolome of Cotton Seedlings under Salt Stress. *Int. J. Mol. Sci.* **2022**, *23*, 9456. [CrossRef]
28. Semenov, A.; Sakhno, T.; Semenova, K. Influence of UV radiation on physical and biological properties of rapeseed in pre-sowing treatment. *Int. J. Innov. Technol. Explor. Eng.* **2021**, *10*, 217–223. [CrossRef]
29. Klymchuk, D.; Kordyum, E.; Vorobyova, T.; Chapman, D.; Brown, C. Changes in vacuolation in the root apex cells of soybean seedlings in microgravity. *Adv. Space Res.* **2003**, *31*, 2283–2288. [CrossRef]
30. Abbasi, G.H.; Akhtar, J.; Anwar-Ul-Haq, M.; Malik, W.; Ali, S.; Chen, Z.-H.; Zhang, G. Morpho-physiological and micrographic characterization of maize hybrids under NaCl and Cd stress. *Plant Growth Regul.* **2015**, *75*, 115–122. [CrossRef]

31. Wassef, E.A.; Wahbi, O.M.; Saqr, E.M.; Saleh, N.E. Response of European seabass (*Dicentrarchus labrax*) to canola oil diets: Effect on growth performance, fish health and liver and intestine histomorphology. *Aquac. Int.* **2016**, *24*, 1073–1088. [CrossRef]
32. Torrecillas, S.; Caballero, M.J.; Montero, D.; Sweetman, J.; Izquierdo, M. Combined effects of dietary mannan oligosaccharides and total fish oil substitution by soybean oil on European sea bass (*Dicentrarchus labrax*) juvenile diets. *Aquac. Nutr.* **2016**, *22*, 1079–1090. [CrossRef]
33. Adesina, S. Assessment of organosomatic indices and histopathological changes in vital organs of *Clarias gariepinus* juveniles fed graded levels of boiled sunflower (*Helianthus annuus*) seed meal. *Ife J. Sci.* **2017**, *19*, 85. [CrossRef]
34. Herak, D.; Kabutey, A.; Divisova, M.; Svatonova, T. Comparison of the Mechanical Behaviour of Selected Oilseeds under Compression Loading. *Not. Bot. Horti Agrobot. Cluj-Napoca* **2012**, *40*, 227–232. [CrossRef]
35. Memete, A.R.; Teusdea, A.C.; Timar, A.V.; Vuscan, A.N.; Mintaș, O.S.; Cavalu, S.; Vicas, S.I. Effects of Different Edible Coatings on the Shelf Life of Fresh Black Mulberry Fruits (*Morus nigra* L.). *Agriculture* **2022**, *12*, 1068. [CrossRef]
36. Sincik, M.; Goksoy, A.T. Investigation of Correlation between Traits and Path Analysis of Confectionary Sunflower Genotypes. *Not. Bot. Horti Agrobot. Cluj-Napoca* **2014**, *42*, 227–231. [CrossRef]
37. Gholinezhad, E.; Darvishzadeh, R.; Bernousi, I. Evaluation of Drought Tolerance Indices for Selection of Confectionery Sunflower (*Helianthus anuus* L.) Landraces under Various Environmental Conditions. *Not. Bot. Horti Agrobot. Cluj-Napoca* **2014**, *42*, 187–201. [CrossRef]
38. Janick, J. Iconography of domesticated sunflower. *Not. Bot. Horti Agrobot. Cluj-Napoca* **2020**, *48*, 1116–1129. [CrossRef]
39. Krupa-Małkiewicz, M.; Kosatka, A.; Smolik, B.; Sędzik, M. Induced Mutations through EMS Treatment and In Vitro Screening for Salt Tolerance Plant of Petunia × atkinsiana D. Don. *Not. Bot. Horti Agrobot. Cluj-Napoca* **2017**, *45*, 190–196. [CrossRef]
40. Puchtler, H.; Sweat Waldrop, F.; Conner, H.M.; Terry, M.S. Carnoy fixation: Practical and theoretical considerations. *Histochemie* **1968**, *16*, 361–371. [CrossRef]
41. Sarac, I.; Bonciu, E.; Butnariu, M.; Petrescu, I.; Madosa, E. Evaluation of the cytotoxic and genotoxic potential of some heavy metals by use of Allium test. *Caryologia Int. J. Cytol.* **2019**, *72*, 37–43. [CrossRef]
42. Biesterfeld, S.; Beckers, S.; Del Carmen Villa Cadenas, M.; Schramm, M. Feulgen staining remains the gold standard for precise DNA image cytometry. *Anticancer. Res.* **2011**, *31*, 53–58.
43. Reisen, D.; Marty, F.; Leborgne-Castel, N. New insights into the tonoplast architecture of plant vacuoles and vacuolar dynamics during osmotic stress. *BMC Plant Biol.* **2005**, *5*, 13. [CrossRef] [PubMed]
44. Niu, X.; Damsz, B.; Kononowicz, A.K.; Bressan, R.A.; Hasegawa, P.M. NaCl-Induced Alterations in Both Cell Structure and Tissue-Specific Plasma Membrane H+ -ATPase Gene Expression. *Plant Physiol.* **1996**, *111*, 679–686. [CrossRef] [PubMed]
45. Laveau, J.H.; Schneider, C.; Berville, A. Microsporogenesis Abortion in Cytoplasmic Male Sterile Plants from *H. petiolaris* or *H. petiolaris* fallax Crossed by Sunflower (*Helianthus annuus*). *Ann. Bot.* **1989**, *64*, 137–148. [CrossRef]
46. Pekol, S.; Baloğlu, M.C.; Altunoğlu, Y. Evaluation of genotoxic and cytologic effects of environmental stressin wheat species with different ploidy levels. *Turk. J. Biol.* **2016**, *40*, 580–588. [CrossRef]
47. Zheng, Y.; Zhang, H.; Deng, X.; Liu, J.; Chen, H. The relationship between vacuolation and initiation of PCD in rice (*Oryza sativa*) aleurone cells. *Sci. Rep.* **2017**, *7*, 41245. [CrossRef]
48. Shan, F.; Wu, Y.; Du, R.; Yang, Q.; Liu, C.; Wang, Y.; Zhang, C.; Chen, Y. Evolutionary analysis of the OSCA gene family in sunflower (*Helianthus annuus* L.) and expression analysis under NaCl stress. *PeerJ* **2023**, *11*, e15089. [CrossRef]
49. Çavuşoğlu, D.; Tabur, S.; Çavuşoğlu, K. The Effects of *Aloe vera* L. Leaf Extract on Some Physiological and Cytogenetical Parameters in *Allium cepa* L. Seeds Germinated under Salt Stress. *Cytologia* **2016**, *81*, 103–110. [CrossRef]
50. Prajapati, P.; Gupta, P.; Kharwar, R.N.; Seth, C.S. Nitric oxide mediated regulation of ascorbate-glutathione pathway alleviates mitotic aberrations and DNA damage in *Allium cepa* L. under salinity stress. *Int. J. Phytoremediation* **2023**, *25*, 403–414. [CrossRef]
51. Jiang, Y.-T.; Yang, L.-H.; Ferjani, A.; Lin, W.-H. Multiple functions of the vacuole in plant growth and fruit quality. *Mol. Hortic.* **2021**, *1*, 4. [CrossRef]
52. Affenzeller, M.J.; Darehshouri, A.; Andosch, A.; Lütz, C.; Lütz-Meindl, U. Salt stress-induced cell death in the unicellular green alga Micrasterias denticulata. *J. Exp. Bot.* **2009**, *60*, 939–954. [CrossRef]
53. Darehshouri, A.; Affenzeller, M.; Lütz-Meindl, U. Cell death upon H_2O_2induction in the unicellular green alga *Micrasterias*. *Plant Biol.* **2008**, *10*, 732–745. [CrossRef]
54. Anido-Varela, L.; Seoane, M.; Esperanza, M.; Cid, A.; Rioboo, C. Cytotoxicity of BP-3 and BP-4: Blockage of extrusion pumps, oxidative damage and programmed cell death on Chlamydomonas reinhardtii. *Aquat. Toxicol.* **2022**, *251*, 106285. [CrossRef] [PubMed]
55. Damsz, B.; Matsumoto, T.K.; Reddy, M.P.; Rus, A.M.; Ibeas, J.I.; Narasimhan, M.L.; Bressan, R.A.; Hasegawa, P.M.; Huh, G.-H. Salt causes ion disequilibrium-induced programmed cell death in yeast and plants. *Plant J.* **2002**, *29*, 649–659. [CrossRef]
56. Beers, E.P.; McDowell, J.M. Regulation and execution of programmed cell death in response to pathogens, stress and developmental cues. *Curr. Opin. Plant Biol.* **2001**, *4*, 561–567. [CrossRef]
57. Assaha, D.V.M.; Ueda, A.; Saneoka, H.; Al-Yahyai, R.; Yaish, M.W. The role of Na+ and K+ transporters in salt stress adaptation in glycophytes. *Front. Physiol.* **2017**, *8*, 509. [CrossRef]
58. Mansour, M.M.F. Role of Vacuolar Membrane Transport Systems in Plant Salinity Tolerance. *J. Plant Growth Regul.* **2023**, *42*, 1364–1401. [CrossRef]

59. Wang, N.; Qi, H.; Qiao, W.; Shi, J.; Xu, Q.; Zhou, H.; Yan, G.; Huang, Q. Cotton (*Gossypium hirsutum* L.) genotypes with contrasting K+/Na+ ion homeostasis: Implications for salinity tolerance. *Acta Physiol. Plant.* **2017**, *39*, 77. [CrossRef]
60. Bogoutdinova, L.R.; Lazareva, E.M.; Chaban, I.A.; Kononenko, N.V.; Dilovarova, T.; Khaliluev, M.R.; Kurenina, L.V.; Gulevich, A.A.; Smirnova, E.A.; Baranova, E.N. Salt Stress-Induced Structural Changes Are Mitigated in Transgenic Tomato Plants Over-Expressing Superoxide Dismutase. *Biology* **2020**, *9*, 297. [CrossRef] [PubMed]
61. Bogoutdinova, L.R.; Baranova, E.N.; Kononenko, N.V.; Chaban, I.A.; Konovalova, L.N.; Gulevich, A.A.; Lazareva, E.M.; Khaliluev, M.R. Characteristics of Root Cells during In Vitro Rhizogenesis under Action of NaCl in Two Tomato Genotypes Differing in Salt Tolerance. *Int. J. Plant Biol.* **2023**, *14*, 104–119. [CrossRef]
62. Youssef, K.; Roberto, S.R.; de Oliveira, A.G. Ultra-Structural Alterations in *Botrytis cinerea*—The Causal Agent of Gray Mold—Treated with Salt Solutions. *Biomolecules* **2019**, *9*, 582. [CrossRef]
63. Sergienko, O.V.; Khalilova, L.A.; Orlova, Y.V.; Shuvalov, A.V.; Myasoedov, N.A.; Karpichev, I.V. Mutation of the ARA7/AtRabF2b Gene, That Increases the Content of the Ara7 Protein Regulating Endocytic Trafficking Pathways, Improves Salt Tolerance of the *Arabidopsis thaliana* (L.) Heynh Plants. *Russ. J. Plant Physiol.* **2022**, *69*, 11. [CrossRef]
64. Jiang, W.; Liu, D. Pb-induced cellular defense system in the root meristematic cells of *Allium sativum* L. *BMC Plant Biol.* **2010**, *10*, 40. [CrossRef] [PubMed]
65. Sharma, S.S.; Dietz, K.-J.; Mimura, T. Vacuolar compartmentalization as indispensable component of heavy metal detoxification in plants: Vacuolar functions in HM detoxification. *Plant Cell Environ.* **2016**, *39*, 1112–1126. [CrossRef] [PubMed]
66. Sychta, K.; Słomka, A.; Kuta, E. Insights into Plant Programmed Cell Death Induced by Heavy Metals—Discovering a *Terra Incognita*. *Cells* **2021**, *10*, 65. [CrossRef]
67. Kar, R.; Singha, P.K.; Venkatachalam, M.A.; Saikumar, P. A novel role for MAP1 LC3 in nonautophagic cytoplasmic vacuolation death of cancer cells. *Oncogene* **2009**, *28*, 2556–2568. [CrossRef]
68. Ohoka, N.; Nagai, K.; Shibata, N.; Hattori, T.; Nara, H.; Cho, N.; Naito, M. SNIPER(TACC3) induces cytoplasmic vacuolization and sensitizes cancer cells to Bortezomib. *Cancer Sci.* **2017**, *108*, 1032–1041. [CrossRef]
69. Levene, A.P.; Goldin, R.D. Physiological hepatic nuclear vacuolation-how long does it persist? *Histopathology* **2010**, *56*, 426–429. [CrossRef]
70. Sharma, S.; Ghufran, S.M.; Ghose, S.; Biswas, S. Cytoplasmic vacuolation with endoplasmic reticulum stress directs sorafenib induced non-apoptotic cell death in hepatic stellate cells. *Sci. Rep.* **2021**, *11*, 3089. [CrossRef]